Journal of Magnetism and Magnetic Materials 471 (2019) 169–176

Contents lists available at ScienceDirect

Journal of Magnetism and Magnetic Materials

journal homepage: www.elsevier.com/locate/jmmm

Research articles

Destroying activity of glycine coated magnetic nanoparticles on lysozyme, α-lactalbumin, insulin and α-crystallin amyloid fibrils

Andrea Antosova[a], Zuzana Bednarikova[a], Martina Koneracka[a], Iryna Antal[a], Vlasta Zavisova[a], Martina Kubovcikova[a], Josephine W. Wu[b], Steven S.-S. Wang[c,*], Zuzana Gazova[a,*]

[a] Institute of Experimental Physics, Slovak Academy of Sciences, Kosice, Slovakia
[b] Department of Optometry, Yuanpei University of Medical Technology, Hsinchu City 30015, Taiwan
[c] Department of Chemical Engineering, National Taiwan University, Taipei 10617, Taiwan

ARTICLE INFO

Keywords:
Amyloid fibrils
Magnetic nanoparticles
Lysozyme
α-Lactalbumin
Insulin
α-Crystallin

ABSTRACT

A great variety of human protein deposition and protein aggregation diseases (Alzheimer's disease, diabetes mellitus, cataract, systemic amyloidosis and other) have been associated with the accumulation of amyloid fibrils in different tissues. Therefore, development of the agents able to reduce amyloid deposits represents an attractive strategy for their treatment. We have investigated ability of glycine coated magnetic nanoparticles (Gly-MNPs) to destroy protein amyloid fibrils. The properties of Gly-MNPs were characterized with the aim to identify the optimized conditions for the glycine adsorption on surface of MNPs. It was found that Gly-MNPs have superparamagnetic behavior and their size, isoelectric point and stability depend on the amount of the glycine in the samples. The obtained results suggest that optimal weight ratio (w/w) for the modification of MNPs by glycine (Gly/Fe_3O_4) is equal to 5/1. The selected Gly_5-$MNPs_1$ were used for the study of their effect on amyloid fibrils of four globular proteins, namely lysozyme, bovine α-lactalbumin, insulin and α-crystallin. It was found that Gly_5-$MNPs_1$ destroy lysozyme, α-lactalbumin and insulin amyloid fibrils in concentration dependence manner. However, Gly_5-$MNPs_1$ were not able significantly destroy bovine α-crystallin amyloid fibrils. We assume that obtained results represent important contribution for rational design of potential therapeutics of amyloid diseases based on nanoparticles.

1. Introduction

Protein amyloid fibrils are highly ordered, insoluble and very stable nanostructures associated with more than 50 amyloid diseases such as Alzheimer's and Parkinson's diseases, diabetes mellitus and others [1–4]. In these diseases the normally soluble proteins are transforming into amyloid aggregates characteristic of high content of cross β-sheet structure. The deposition of poly/peptides in amyloid form is the main cause of human organs and tissues damage [5]. It seems that under appropriate conditions every poly/peptide has propensity to self-assembly into amyloid structures; therefore, formation of amyloid fibrils is generic property of poly/peptide chain [6–8].

There are several globular proteins with high propensity to form amyloid fibrils. The amyloid aggregation of human lysozyme, a bacteriolytic enzyme presented in the liver, milk, saliva and serum, is associated with fatal hereditary systemic lysozyme amyloidosis [9,10]. Hen egg white lysozyme (HEWL) is often used to investigate the lysozyme amyloid self-assembly as it is highly homologous to human variant [11,12]. HEWL is a protein consisting of 129 amino acids (14.7 kDa) and its physico-chemical properties are well characterized [9]. The α-lactalbumin, 123 amino acids (14.17 kDa) protein, is a predominant protein component of milk and the second most abundant protein in whey [13]. α-Lactalbumin can evoke a variety of physiological effects [14] such as modulation of the lactose synthase activity or apoptotic activity in tumor cells [15,16]. Till now the self-assembly of α-lactalbumin was not associated to any specific amyloid disease. Insulin is a small globular 51 amino acids (5.8 kDa) protein hormone that is crucial for control of the glucose metabolism and diabetes treatment. Insulin amyloid deposits have been found in the sites of subcutaneous drug application in patients with long-term diabetes treatment. Insulin amyloid aggregation causes also a serious problem in the production, storage and delivery of this important biopharmaceutical compound as well as in application of the insulin pumps [17]. The α-crystallins are large complex proteins (~700 kDa) primarily found within the mammalian eye lens where they contribute to lens transparency and refractive properties [18]. Crystallin aggregation is the most important

* Corresponding authors.
E-mail addresses: sswang@ntu.edu.tw (S. S.-S. Wang), gazova@saske.sk (Z. Gazova).

https://doi.org/10.1016/j.jmmm.2018.09.096
Received 22 June 2018; Received in revised form 21 August 2018; Accepted 24 September 2018
Available online 25 September 2018
0304-8853/

factor in cataract formation [19]. With ageing of the lens, α-crystallin is post-translation modified, unfolded and aggregated into amorphous and/or amyloid fibrils. Factors that lead to protein aggregation include mutations in crystallin proteins, which are known to cause congenital cataracts or oxidative stress, which in turn contributes to age related cataracts [20–22].

Since the presence of amyloid fibrillar deposits is the main hallmark of amyloid diseases, development of the agents able to combat them is one of key approaches for their treatment. In last decade, various molecules with ability to inhibit amyloid fibrillization or destroy amyloid fibrils have been found. The anti-amyloid properties were observed for small molecules, peptides, antibodies or heat shock proteins [23–25]. Recently, the nanoparticles have been suggested as one of a possible agent affecting amyloid aggregation. It is mainly due to their unique properties as high surface/volume ratio and possibility of various surface modification providing large and specific surface areas for interaction with biomacromolecules [26,27]. It was found that copolymer or cerium nanoparticles or quantum dots significantly enhance the rate of fibril formation [28]. While gold nanoparticles have been reported to induce formation of protein aggregates [29], the ablation of amyloid aggregates by gold nanoparticles has also been observed [30,31]. The anti-amyloid activities were found for fluorinated nanoparticles [32] as well as for fullerenol [33].

The magnetic properties, relative high biocompatibility and low toxicity increase application of magnetic nanoparticles (MNPs) in biomedicine as in magnetic resonance imaging, drug delivery, bioseparation and hyperthermia [34–37]. However, there are only few reports on the interaction of the magnetic nanoparticles with amyloid aggregation of poly/peptides. Mahmoudi et al. investigated controversy effect of magnetic nanoparticles on kinetic of Aβ fibrillization. While lower concentrations of superparamagnetic nanoparticles inhibited fibrillation, higher concentrations increased the rate of Aβ fibrillation [38]. Sen et al. found that $MnFe_2O_4$ nanoparticles inhibit fibrillation of human serum albumin [39]. The fluorescent MNPs were also used for detection of Aβ plaques and their removal by magnetic field [40]. Wang et al. reported that the heparin-functionalized magnetic glyconanoparticles can bind to Aβ, induce the formation of fibrils, and protect neuronal cells from Aβ induced cell death [41]. In our previous studies we have found that Fe_3O_4-based nanoparticles are able to reduce amyloid aggregation of lysozyme or insulin [42–44].

The aim of the present study was characterization of the properties of the prepared glycine (Gly) coated magnetic nanoparticles and identification of the optimized conditions for the adsorption of glycine on MNPs. It was found that Gly-MNPs have superparamagnetic behavior and their size, isoelectric point and stability depend on the amount of the glycine in samples. The obtained results suggest that optimal weight ratio (w/w) for the modification of MNPs by glycine (Gly/Fe_3O_4) was equal to 5/1. The selected Gly_5-$MNPs_1$ were used for the study of their effect on amyloid fibrils of four proteins, namely lysozyme, α-lactalbumin, insulin and α-crystallin. We have found that Gly_5-$MNPs_1$ destroy lysozyme, α-lactalbumin and insulin amyloid fibrils in concentration dependence manner. However, Gly_5-$MNPs_1$ were not able significantly destroy bovine α-crystallin amyloid fibrils. We assume that obtained results represent important contribution for rational design of potential therapeutics of amyloid diseases based on nanoparticles.

2. Experiment

2.1. Materials

Glycine (Gly) (99%), ferric chloride hexahydrate ($FeCl_3{\cdot}6H_2O$), ferrous sulfate heptahydrate ($FeSO_4{\cdot}7H_2O$), ammonium hydroxide (NH_4OH), perchloric acid ($HClO_4$), lysozyme from hen egg-white (lyophilized powder, lot number L 6876, ~40.000 units/mg protein), α-lactalbumin from bovine milk (type III, calcium depleted, purity ≥85%, L6010), insulin (human recombinant insulin, expressed in yeast, lot number I2643, ~24 IU/mg protein), α-crystallin from bovine eye lens (C4163, purity ≥70%), NaCl, glycine (Gly), HCl, trifluoroethanol (TFE) and thioflavin T (ThT) were obtained from Sigma Aldrich Chemical Company (St. Louis, MO). The protein concentrations were determined spectrophotometrically (UV VIS JASCO V-630 spectrophotometer) using an extinction coefficient measured at λ = 280 nm. Ultrapure deionized water (Milli-Q) was used throughout the experiments.

2.2. Preparation of Fe_3O_4 nanoparticles stabilized in $HClO_4$ and their functionalization with glycine

Iron oxide (Fe_3O_4) magnetic nanoparticles (MNPs) were synthesized by co-precipitation method and stabilized with perchloric acid by the method described by Antal et al. [42,45,46]. The concentration of Fe_3O_4 in prepared aqueous solution of MNPs was estimated by thiocyanate colorimetry [47] and was equal to 30 mg/mL. The functionalization of iron oxide MNPs with amino acid glycine to obtain the Gly-MNPs was carried out by mixing of glycine aqueous solution (c_{Gly} = 100 mg/mL) with nanosuspension of MNPs at different weight ratio (w/w) of Gly/Fe_3O_4 ranging from 0 to 50 during 72 h at 25 °C. The samples were centrifuged at 35,000 rpm for 20 min to separate unbound amino acid. For determination of Gly concentration in supernatants the spectrophotometric method (described below) was used. Bound amount of Gly was then calculated as difference between total and unbound amount of Gly.

2.3. UV/VIS spectroscopy

The adsorption of Gly onto the MNPs surface was quantified using the spectrophotometric method with ninhydrin using SPECORD® PC 40 UV VIS spectrophotometer [48]. To obtain the calibration curve, amino acid solutions with different volumes (0.1–0.45 mL) were put to the test tubes. Then the distilled water was added to the all tubes to make up the 4 mL volume. As a blank the distilled water was used. In the next step, 1 mL of 2% w/v ninhydrin reagent was added to all the test tubes and stirred using vortex. The tubes were placed in thermomixer for 15 min at the temperature 100 °C and subsequently cooled in cold water. After addition of 1 mL of ethanol/water (1:1) the mixtures were mixed and the absorbance at 570 nm was recorded for each sample. The same procedure was used to determine Gly concentrations in supernatants.

2.4. Nanoparticles characterization

Zetasizer NanoZS (Malvern Instruments) was used for determination of hydrodynamic size distribution of MNPs and Gly-MNPs using the dynamic light scattering method (DLS) with a scattering angle of 173° as well as for zeta potential measurements. Zeta potential is commonly used to predict and control the stability of the sample. It is proportional to electrophoretic mobility that is determined by Laser Doppler Velocimetry.

Scanning electron microscopy (SEM, JEOL 7000F microscope) was used for characterization of the morphology of both MNPs and Gly-MNPs. The samples were prepared by deposition of the sample containing MNPs or Gly-MNPs on a double sided carbon tape stuck on the SEM sample stub and dried under vacuum prior to sputtering with carbon and subsequent observation.

The field dependent magnetization measurements were carried out using Magnetic Property Measuring System model MPMS-XL-5 (Quantum Design) equipped with 5 T superconducting magnet.

2.5. Formation of protein amyloid fibrils

Amyloid fibrillization of lysozyme (LF) – Lysozyme was dissolved to a final concentration of 5 mg/mL in 70 mM glycine buffer containing

80 mM NaCl at pH 2.7. To produce the amyloid fibrils, the solution of lysozyme was incubated at 65 °C and stirred constantly (1200 rpm) for 2 h.

Amyloid fibrillization of α-lactalbumin (LAF) – α-Lactalbumin was dissolved to a final concentration of 5 mg/mL in 100 mM NaCl at pH 2.0. Formation of amyloid fibrils was achieved by incubation of the solution at 60 °C and constant stirring (1200 rpm) for 5 h.

Amyloid fibrillization of insulin (IF) – Insulin at final concentration of 2 mg/mL in 100 mM NaCl at pH 1.6 was incubated at 65 °C and stirred constantly (1200 rpm) for 2 h.

Amyloid fibrillization of α-crystallin (CRF) The solution of α-crystallin at final concentration of 10 mg/mL in 10% trifluoroethanol (TFE) was incubated at 60 °C and constantly stirred (1200 rpm) for 4 h. The pH of the solution was adjusted with HCl to 2.0.

The formation of amyloid fibrils was confirmed using ThT assay and atomic force microscopy.

2.6. Thioflavin T (ThT) fluorescence assay

The formation of amyloid fibrils was monitored by characteristic changes in ThT fluorescence intensity. ThT was added to studied lysozyme, α-lactalbumin and insulin samples (10 μM) to a final concentration of 20 μM and samples were incubated at 37 °C for 1 h. In the case of α-crystallin the concentration of 0.7 μM protein and 70 μM ThT were used. Fluorescence intensity was measured in a black 96-well plate using a Synergy Mx (BioTek Company, USA) spectrofluorimeter. The excitation wavelength was set at 440 nm and the emission recorded at 485 nm. The emission/excitation slits were adjusted to 9.0/9.0 nm and the top probe vertical offset was 6 nm. All ThT fluorescence experiments were performed in triplicate and the final value is the average of measured values.

2.7. Interference of Gly-MNPs with protein amyloid fibrils

ThT fluorescence assay was used to investigate the interaction of glycine coated MNPs with amyloid fibrils of studied proteins. The nanoparticles with w/w ratio of Gly to Fe_3O_4 = 5/1 (Gly_5-$MNPs_1$) were selected for this study. Destroying activities were measured after 24 h incubation of Gly_5-$MNPs_1$ with LF (10 μM = 0.147 mg/mL), LAF (10 μM = 0.142 mg/mL), IF (10 μM = 0.058 mg/mL) and CRF (0.7 μM = 0.490 mg/mL) at 37 °C. The concentration ratios of fibrils to Gly_5-$MNPs_1$-Fe_3O_4 were ranging from 20:1 to 1:20. The values of fluorescence intensities were normalized to the fluorescence signal detected for untreated amyloid fibrils (taken as 100%). Each experiment was performed in triplicates and values represent the average of the obtained values. As a control, the ThT fluorescence intensities of Gly_5-$MNPs_1$ in buffer were measured. The DC_{50} values (concentration of Gly_5-$MNPs_1$ causing 50% destroying of fibrils) were obtained by fitting the average values by a nonlinear least-squares method with the sigmoidal hill 3 parameters equation ($y = a/[1 + (x/x_0)b]$).

2.8. Atomic force microscopy (AFM)

Morphology of fibrils was examined using atomic force microscopy. Samples for AFM were prepared by drop casting of 10 μL aliquots on the surface of freshly cleaved mica and after 10 min adsorption they were rinsed with ultrapure water and left air dried. AFM images were taken using a Scanning Probe Microscope (Veeco diInnova) in a tapping mode under ambient conditions using rectangular uncoated silicon cantilever NCHV (Bruker AFM Probes with a specific resistance of 0.01–0.025 Ω cm, antimony (n) doped Si) with a typical resonance frequency 320 kHz and a force constant 42 N/m. No smoothing or noise reduction was applied.

3. Results and discussion

Due to the unique properties of magnetic nanoparticles as large surface area, small size, superparamagnetic properties and stability they are useful in a wide range of applications. For biomedical applications the MNPs are usually coated with biological molecules to increase their biocompatibility. In our study we have identified the optimized conditions for the adsorption of amino acid glycine on MNPs and characterized their physico-chemical properties. Moreover, we investigated the interference of glycine coated magnetic nanoparticles with amyloid fibrils of studied proteins.

The perchloric stabilized iron oxide magnetic nanoparticles MNPs were synthesized by co-precipitation standard method [42,46]. To find the optimal conditions for MNPs coating with glycine we used a wide concentration range of amino acid to get the w/w ratio of Gly/Fe_3O_4 from 0.05/1 to 62/1 (the concentration of Fe_3O_4 was equal to 1.5 mg/mL). The physico-chemical properties of the MNPs or Gly-MNPs coated with different amount of glycine were examined using various methods. The size and zeta potential were measured using Zetasizer NanoZS and obtained data are presented in Fig. 1A. The hydrodynamic size of Gly-MNPs slightly changes for Gly/Fe_3O_4 ratios from 0.05/1 to 10/1 (Fig. 1A, diamonds). The size distribution of the Gly-MNPs was narrow; the polydispersity index from DLS was < 0.2 (data not shown). For this range the high values of zeta potential (approximately +47 mV) indicate the high surface charge and good colloidal stability of Gly-MNPs (Fig. 1A, circles). Starting with the Gly/Fe_3O_4 weight ratio greater than 11/1 the Gly-MNPs samples sediment (Fig. 1B) due to the loss of their colloidal stability. The absolute value of the zeta potential begins to decrease because the electrostatic stabilization of Gly-MNPs is less effective which is also manifested in an increase in hydrodynamic size up to 550 nm.

Moreover, the zeta potential of the Gly-MNPs was measured and obtained dependence of isoelectric point (IEP – Value of pH when the electrical charge density on the nanoparticles surface is zero) *vs.* Gly/Fe_3O_4 weight ratio is displayed in Fig. 2A. The data clearly show that IEP value is about 6.8 for Gly-MNPs with w/w ratio ranging from 0.05/1 to 5/1. The further increase of the Gly concentration leads to significant decrease of IEP value. The obtained data were fitted and from curve the optimal theoretical weight ratio of Gly/Fe_3O_4 was determined as 5/1.

Zeta potential of MNPs and Gly-MNPs (with the weight ratio of Gly/Fe_3O_4 = 5/1) colloid solutions was measured as a function of pH (Fig. 2B). The observed IEP value of MNPs (pH ~ 6.8) (Fig. 2B squares) is close to 7 and well corresponds to the reported value in the literature [46,49]. The IEP value of Gly-MNPs is slightly shifted to lower values of pH ~ 6.6 (Fig. 2B circles) [50]. The obtained data indicate that in acidic medium the Gly-MNPs are stable. At pH value higher than 7 they become to be unstable and Gly can be partially desorbed from the surface of MNPs.

The adsorbed amount of glycine on nanoparticles surface was calculated from difference between the Gly used for modification and Gly assayed in the supernatant. The amount of adsorbed Gly increased with increasing of the amino acid concentration (from 0.15 to 25.2 mg/mL corresponding to the theoretical weight ratio Gly/Fe_3O_4 = 0.1/1–17/1) in the magnetite suspension. The adsorption of Gly on MNPs as well as the optimal theoretical Gly loading was studied using UV–VIS technique (Fig. 3).

The steady-state values determined for Gly concentration from 6.5 mg/mL (Fig. 3A) suggest that further increase of Gly concentration does not lead to increasing of the amount of adsorbed Gly molecules on MNPs surface. The Gly loading concentration of 6.5 mg/mL corresponds to weight ratio Gly/Fe_3O_4 = 5/1. This optimal value of the Gly loading was also confirmed by the relationship of theoretical Gly loading *vs.* Gly entrapment (Fig. 3B). The optimal weight ratio of Gly/Fe_3O_4 equal to 5/1 is in agreement with the measurement of zeta potential and the isoelectric point. These Gly-MNPs are hereinafter referred to as Gly_5-$MNPs_1$.

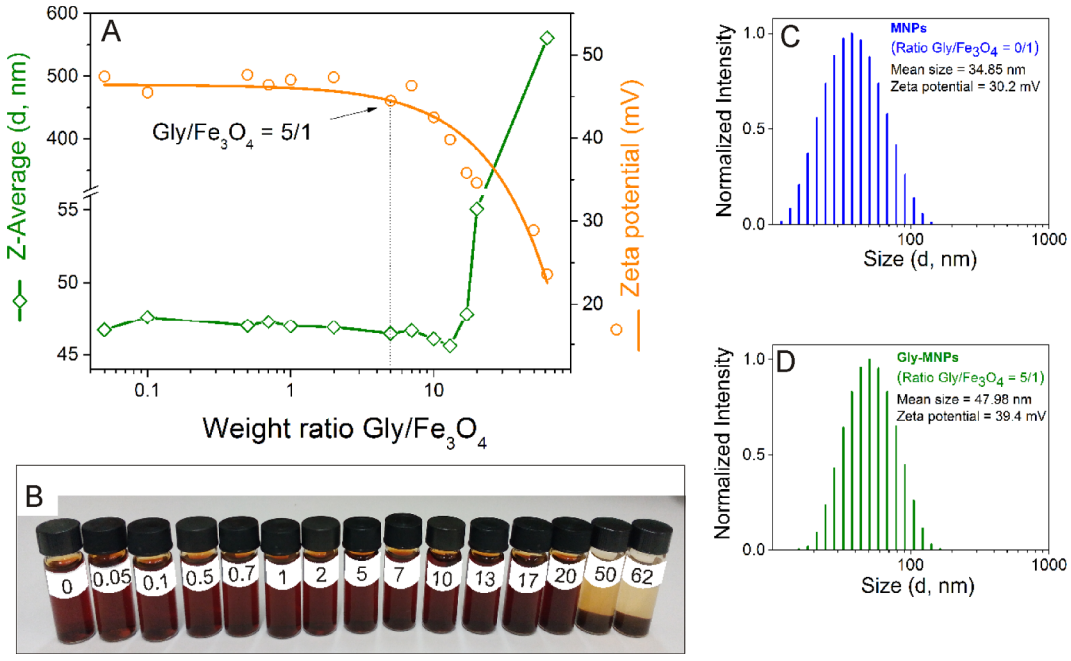

Fig. 1. Effect of different glycine loadings leading to various w/w Gly/Fe_3O_4 ratios (0.05/1 – 62/1) on the average hydrodynamic size of Gly-MNPs and zeta potential (A). Photo of the Gly-MNPs samples with given w/w ratios of Gly/Fe_3O_4 (B). Size distribution of MNPs (C) and Gly-MNPs (D).

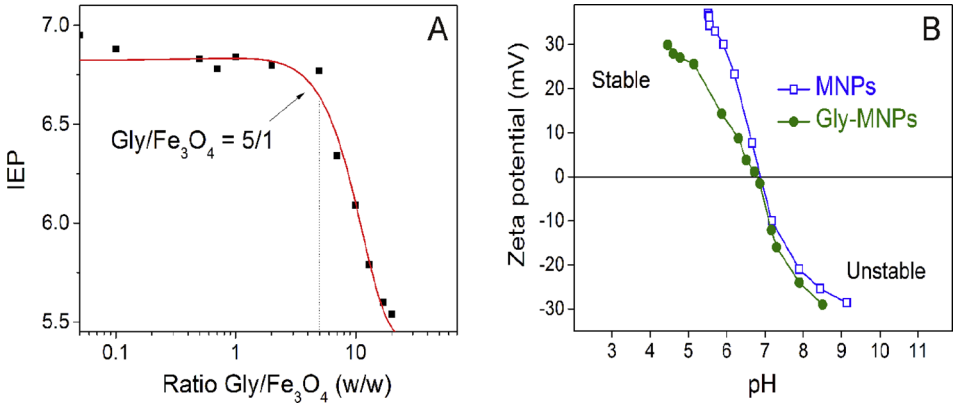

Fig. 2. Dependence of IEP of Gly-MNPs on the weight ratio of Gly/Fe_3O_4 (A). Zeta potential of colloid solutions of MNPs (squares) and Gly-MNPs (circles) with the weight ratio of Gly/Fe_3O_4 = 5/1 as a function of pH (B).

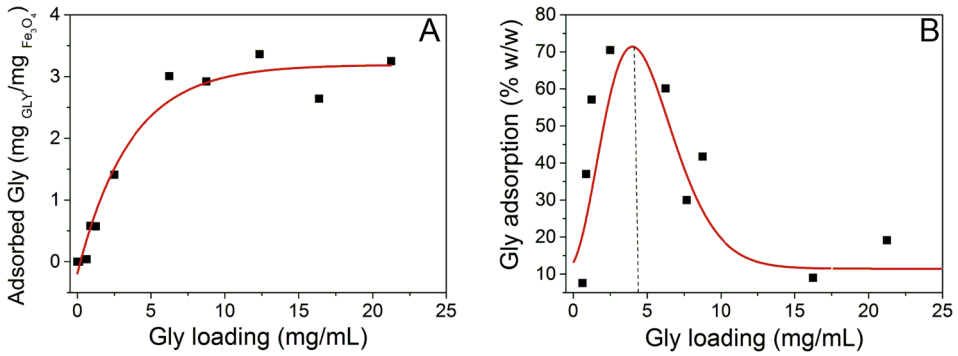

Fig. 3. Adsorption isotherm of Gly on MNPs (A) and effect of various theoretical Gly loadings on Gly adsorption (B).

Next, the morphology of naked MNPs and Gly_5-$MNPs_1$ was observed using microscopic technique SEM. The obtained images are presented in Fig. 4. The SEM image (Fig. 4A) suggests that MNPs are polydisperse with circular morphology and mean magnetic core diameter of 39 nm (Fig. 4B).

The SEM image Gly_5-$MNPs_1$ is shown in Fig. 4C. From this image one can see that particles of Gly_5-$MNPs_1$ sample are roughly spherical with smooth surface. Particle size distributions constructed from SEM images are in the Fig. 4B, D. After Gly coating the mean diameter of MNPs increased from the value 39 to 45 nm.

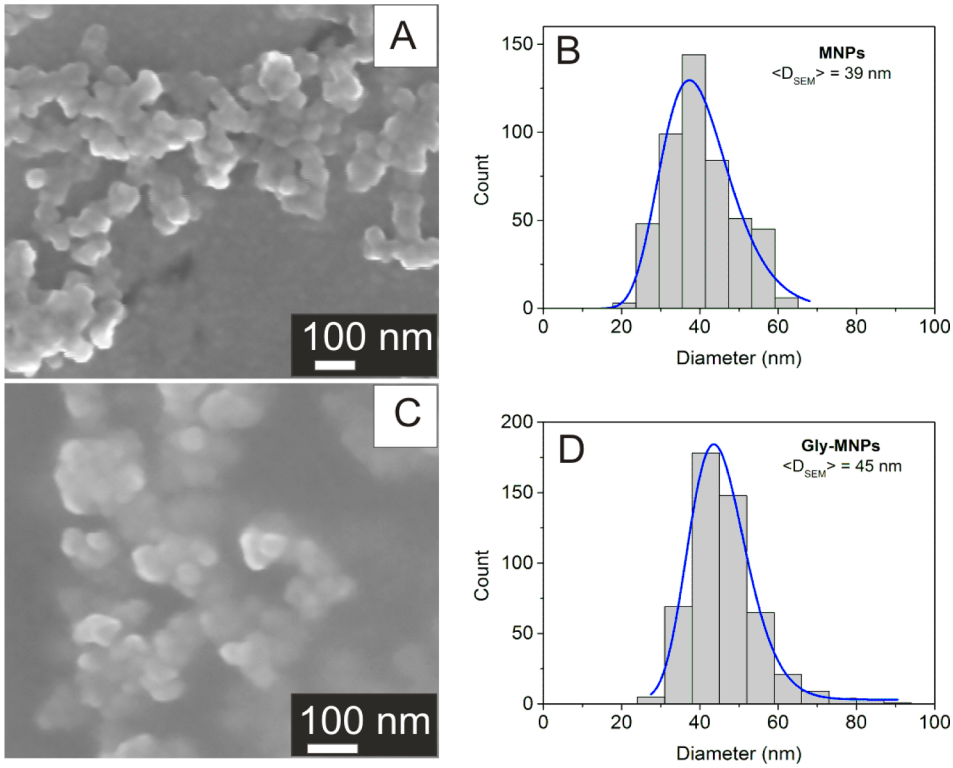

Fig. 4. SEM images of MNPs (A) and Gly_5-$MNPs_1$ (C). Particle size distributions of MNPs (B) and Gly_5-$MNPs_1$ (D) based on SEM images.

Fig. 5. Field-dependent magnetization plots of MNPs and Gly-MNPs (Gly/Fe_3O_4 = 5/1).

The Gly_5-$MNPs_1$ were further used for investigation of their effect on protein amyloid fibrils. We examined the interference of Gly_5-$MNPs_1$ with amyloid fibrils of lysozyme (LF), α-lactalbumin (LAF), insulin (IF) and α-crystallin (CRF). The amyloid fibrils were formed by incubation of soluble proteins at acidic pH, high temperature and under constant stirring.

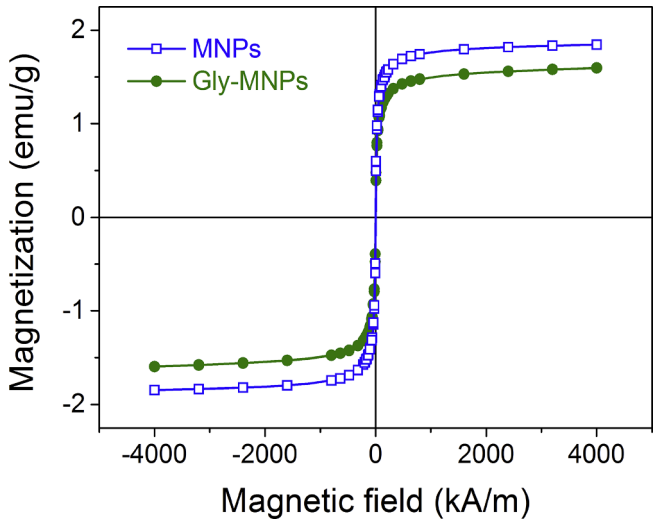

Fig. 5. shows the field dependent magnetization plots of both MNPs and Gly_5-$MNPs_1$ at 300 K. The samples exhibit superparamagnetic behavior without magnetic hysteresis and remanence at 300 K. The maximum magnetizations of MNPs and Gly_5-$MNPs_1$ were found to be 1.8 and 1.5 emu/g at 300 K, respectively. This slight decrease in magnetization can be attributed to the adsorption of Gly molecules on their surface. However, the retention of superparamagnetic property at room temperature and biocompatible amino acid shell makes these nanoparticles suitable for various biomedical applications.

The amyloid character of fibrils was confirmed using ThT fluorescence assay. The transformation of the native forms of proteins into amyloid fibrils is associated with significant increase of ThT fluorescence intensity (Fig. 6). The amyloid morphology of fibrils formed from studied proteins was confirmed using AFM as shown in Fig. 9A, C, E and G.

The incubation of Gly_5-$MNPs_1$ with amyloid fibrils of studied proteins (ratio of fibrils to Gly_5-$MNPs_1$ is 1:2) was studied using ThT assay. The results are presented in Fig. 7. The presence of nanoparticles in case of LF, LAF and IF caused significant decrease in fluorescence intensities

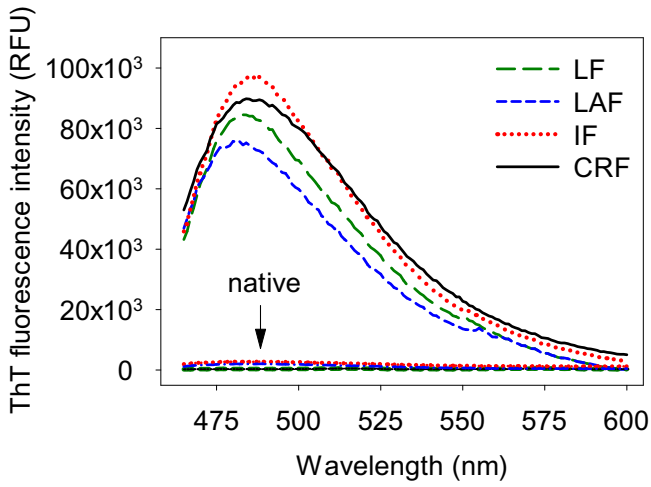

Fig. 6. ThT fluorescence spectra of 10 μM native lysozyme and lysozyme amyloid fibrils (10 μM LF; green dashed line), 10 μM native α-lactalbumin and its amyloid fibrils (10 μM LAF; blue short dashed line), 10 μM insulin in native form and amyloid fibrils (10 μM IF; red dotted line) and 0.7 μM native α-crystallin and after amyloid fibrillization (0.7 μM CRF; black solid line). (For interpretation of the references to colour in this figure legend, the reader is referred to the web version of this article.)

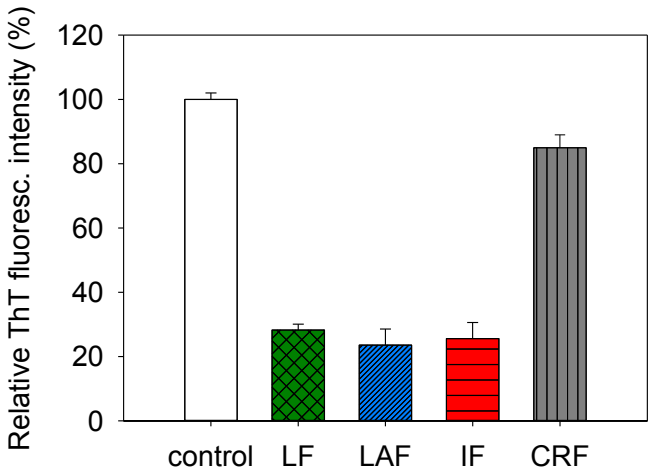

Fig. 7. Effect of Gly_5-$MNPs_1$ on lysozyme (LF), α-lactalbumin (LAF), insulin (IF) and α-crystallin (CRF) amyloid fibrils detected by ThT assay after 24 h incubation. The data were normalized to fluorescence intensity detected for untreated fibrils. Ratio of fibrils to magnetite of Gly_5-$MNPs_1$ was 1: 2.

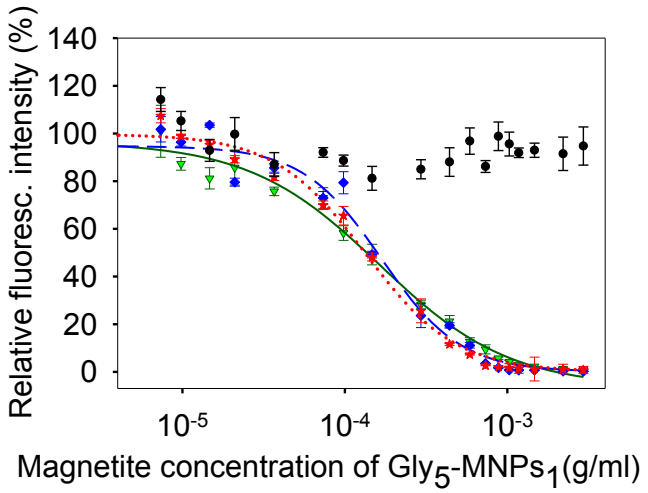

Fig. 8. ThT fluorescence intensities determined for lysozyme (LF-green triangles), α-lactalbumin (LAF-blue diamonds), insulin (IF-red stars) and α-crystallin (CRF-black circles) amyloid fibrils after 24 h incubation with increasing concentration of Gly_5-$MNPs_1$. The fluorescence intensities were normalized to the fluorescence intensity determined for untreated lysozyme fibrils of given protein (taken as 100%). The curves were obtained by fitting the average values by non-linear least-squares method. (For interpretation of the references to colour in this figure legend, the reader is referred to the web version of this article.)

(about 70%) indicating reduction of the amount of amyloid fibrils. Incubation of CRF with Gly_5-$MNPs_1$ led to small decline of the fluorescence intensity about 15% which suggests that these nanoparticles have weak ability to destroy the α-crystallin amyloid fibrils. It must be noted that the fluorescence signal of Gly_5-$MNPs_1$ alone was negligible.

The possible effect of free glycine was also investigated at the same experimental conditions used for Gly_5-$MNPs_1$. It was found that ThT fluorescence intensity in the presence of Gly is comparable to that of fibrils (data not shown). The obtained data suggest that glycine alone has no significant effect on amyloid fibrils of studied proteins.

In order to study the interaction between Gly_5-$MNPs_1$ and LF, LAF, IF and CRF amyloid fibrils in more details the effect of Gly_5-$MNPs_1$ on amyloid fibrils was investigated at different Gly_5-$MNPs_1$ concentrations (ratio of protein fibrils to magnetite of Gly_5-$MNPs_1$ was from 20:1 to 1:20) using ThT assay. The obtained fluorescence intensities are presented in Fig. 8. Interference of Gly_5-$MNPs_1$ with amyloid fibrils of lysozyme (Fig. 8, green triangles), α-lactalbumin (Fig. 8, blue diamond) and insulin (Fig. 8, red stars) led to a steep decline of fluorescence intensities above a threshold concentration of nanoparticles. The fitted fluorescence data were used for calculation of DC_{50} values (concentration of Gly_5-$MNPs_1$ leading to 50% destroying of amyloid fibrils) which are summarized in Table 1. In case of amyloid fibrils of lysozyme and insulin the obtained DC_{50} values are similar and have the lowest values equal to 133.9 μg/mL (LF) and 130.9 μg/mL (IF), respectively. Less efficient destroying ability of Gly_5-$MNPs_1$ was detected for α-lactalbumin amyloid fibrils (DC_{50} = 156.6 μg/mL). The data obtained for α-crystallin amyloid fibrils clearly show that Gly_5-$MNPs_1$ within the studied concentration range are not able significantly destroy CRF (Fig. 8, black circles) as the fluorescence intensities of the samples are comparable to amyloid fibrils alone (taken as 100%). Therefore, the DC_{50} value could not be determined.

In addition to the ThT fluorescence analyses the effect of Gly_5-$MNPs_1$ on studied amyloid fibrils was investigated using atomic force microscopy which allows direct visualization of amyloid structures. The typical morphology of amyloid fibrils was observed for fibrillar aggregates from studied proteins as it is shown in Fig. 9A, C, E and G. The fibrils are unbranched and twisted; however, the length, diameter and tendency to form fibril clusters are changed in dependence on the protein. Lysozyme fibrils are straight fibers (Fig. 9A), amyloid fibrils of α-lactalbumin are shorter and form huge clusters (Fig. 9C) and insulin forms very long fibrils with tendency of lateral association (Fig. 9E). As shown in Fig. 9G α-crystallin fibrillizes to the long and thin unbranched fibrils. The incubation of lysozyme, α-lactalbumin and insulin amyloid

Table 1
DC_{50} values determined after treatment of amyloid fibrils (LF, LAF, IF and CRF) with Gly_5-$MNPs_1$.

Amyloid fibrils	DC_{50} value (μg/mL)
Lysozyme (LF)	133.9 ± 5.26
α-Lactalbumin (LAF)	156.6 ± 3.67
Insulin (IF)	130.9 ± 2.88
α-Crystallin (CRF)	N/A

fibrils with Gly_5-$MNPs_1$ caused significant reduction in the number and size of fibrils (Fig. 9B, D, F). Only very small and thin fibrillar structures can be observed together with globular aggregates. As a result of destroying activity of Gly_5-$MNPs_1$ the insulin fibrils were shorter, their amount was impaired and fragments of fibrils and dotted aggregates can be observed (Fig. 9F). On the other hand, the morphology and amount of CRF before (Fig. 9G) and after treatment with Gly_5-$MNPs_1$ were not changed (Fig. 9H). Thus, the AFM images confirmed data obtained using ThT assay which suggest that Gly_5-$MNPs_1$ are able to destroy amyloid fibrils of lysozyme, α-lactalbumin and insulin; however, this ability is not observed in case of α-crystallin amyloid fibrils.

We suppose that ability of Gly_5-$MNPs_1$ to destroy the amyloid fibrils is caused by adsorption of the nanoparticles on the amyloid fibrils (LF, LAF, IF) allowing the interaction between nanoparticles and hydrophobic residues of the fibrils and thus interrupt the interface between two neighboring β-sheets stabilizing the amyloid fibrils. The similar results were observed also for tyrosine- and tryptophan-coated gold nanoparticles which were able to inhibit amyloid aggregation of insulin [51]. The opposite, non-destroying effect of Gly_5-$MNPs_1$ observed for α-crystallin fibrils can be explained by arrangement of the amino acids within as well as on the surface of the amyloid CRF fibrils. The α-crystallin is a large and due to its chaperon activity also very stable protein. Interestingly, it was found that even in its amyloid form, α-crystallin has its chaperone activity [25]. Due to this, we assume, that α-crystallin amyloid fibrils are more stable than amyloid fibrils formed from other studied proteins and, therefore the Gly_5-$MNPs_1$ are not able to affect the hydrogen bonds forming the β-sheets of fibrils.

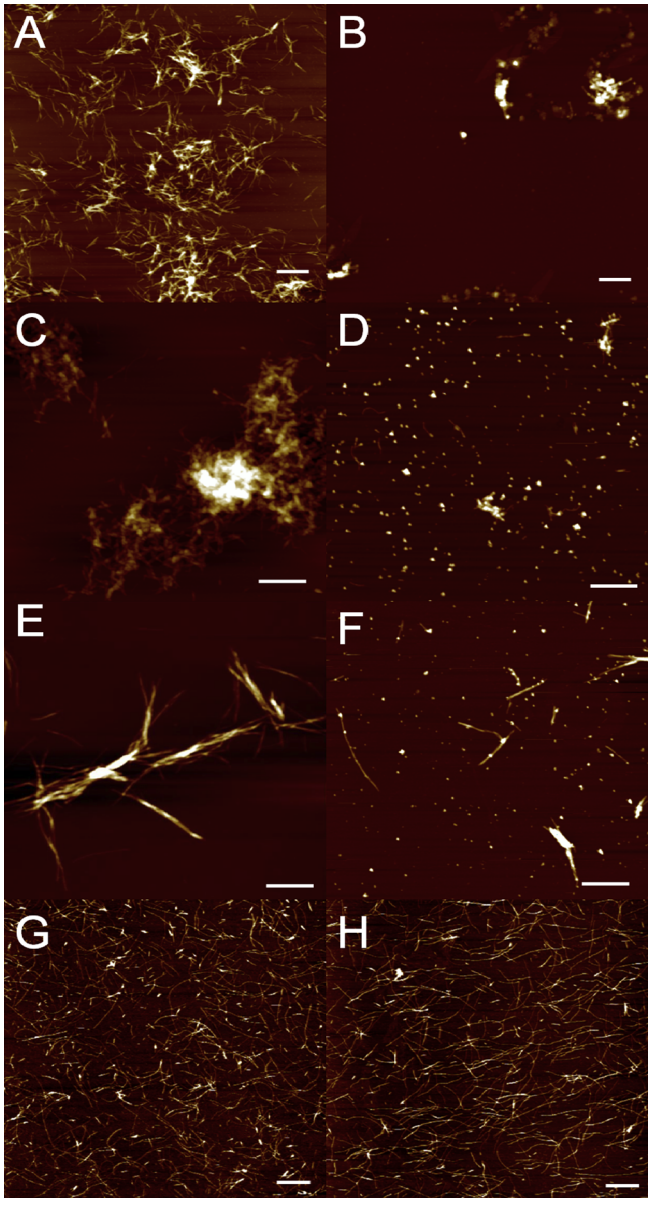

Fig. 9. AFM images of amyloid fibrils of (A) lysozyme (LF), (C) α-lactalbumin (LAF), (E) insulin (IF) and (G) α-crystallin (CRF) and after incubation withGly_5-$MNPs_1$ with (B) LF (D) LAF, (F) IF and (H) CRF. Ratio of fibrils to magnetite of Gly_5-$MNPs_1$ was 1: 2. Scale bar is 1 μm for all images.

4. Conclusion

There are only a few studies related to the effect of superparamagnetic nanoparticles on protein amyloid aggregation despite their wide possible applications in biomedicine. Using several methods we have characterized the properties of the glycine coated magnetic nanoparticles. It was found that Gly-MNPs have superparamagnetic behavior and their size, isoelectric point and stability depend on the amount of the glycine in the sample. The obtained results suggest that optimal weight ratio (w/w) for the modification of MNPs by glycine (Gly/Fe_3O_4) was equal to 5/1 (Gly_5-$MNPs_1$). The selected Gly_5-$MNPs_1$ have different effect on amyloid fibrils of lysozyme, -lactalbumin, insulin and α-crystallin. We have found that Gly_5-$MNPs_1$ destroy lysozyme, α-lactalbumin and insulin amyloid fibrils in concentration dependence manner. The destroying activity determined by DC_{50} values is similar in case of lysozyme and insulin fibrils and is in range of μg/mL. A slight lower destroying ability of nanoparticles was observed in case of α-lactalbumin amyloid fibrils. It is probably caused by interaction of nanoparticles and hydrophobic residues of the fibrils leading to the interruption of the interface between two neighboring β-sheets. The Gly_5-$MNPs_1$ were not able significantly destroy α-crystallin amyloid fibrils. It is probably due to given arrangement of the amino acids within as well as on the surface of α-crystallin amyloid fibrils leading to formation of very stable fibrils. We assume that obtained results represent important contribution for rational design of potential therapeutics of amyloid diseases based on nanoparticles.

Acknowledgements

This work was supported by the research grants Slovak Academy of Sciences, Slovakia – VEGA 2/0145/17 and SAS-MOST JRP 2015/5, Ministry of Science and Technology – Taiwan MOST 105-2923-E-002-010-MY3 and by the Slovak Research and Development Agency, Slovakia under the contracts Nos. APVV-14-0120, APVV-14-0932.

References

[1] J.S. Pedersen, D.E. Otzen, Amyloid—a state in many guises: Survival of the fittest fibril fold, Protein Sci. 17 (2008) 2–10.
[2] J.D. Sipe, A.S. Cohen, Review: history of the amyloid fibril, J. Struct. Biol. 130 (2000) 88–98.
[3] S.L. Gras, Amyloid fibrils: From disease to design. New biomaterial applications for self-assembling cross-β fibrils, Aust. J. Chem. 60 (2007) 333–342.
[4] F. Chiti, C.M. Dobson, Protein misfolding, functional amyloid, and human disease, Annu. Rev. Biochem. 75 (2006) 333–366.
[5] A.D. Wechalekar, J.D. Gillmore, P.N. Hawkins, Systemic amyloidosis, Lancet 387 (2016) 2641–2654.
[6] M. Fandrich, V. Forge, K. Buder, M. Kittler, C.M. Dobson, S. Diekmann, Myoglobin forms amyloid fibrils by association of unfolded polypeptide segments, Proc. Natl. Acad. Sci. U.S.A. 100 (26) (2003) 15463–15468.
[7] L.A. Munishkina, A.L. Fink, V.N. Uversky, Conformational prerequisites for formation of amyloid fibrils from histones, J. Mol. Biol. 342 (4) (2004) 1305–1324.
[8] C.K. Chang, W.A. Chen, C.Y. Sie, S.C. Lin, L.T. Lin, T.H. Lin, C.C. Hsu, S.S. Wang, Investigating the effects of plasma pretreatment on the formation of ordered aggregates of lysozyme, Colloids Surfaces B: Biointerfaces 126 (2015) 154–161.
[9] M. Dumoulin, J.R. Kumita, C.M. Dobson, Normal and aberrant biological self-assembly: insights from studies of human lysozyme and its amyloidogenic variants, Acc. Chem. Res. 39 (2006) 603–610.
[10] L.A. Morozova, J. Zurdo, A. Spencer, W. Noppe, V. Receveur, D.B. Archer, M. Joniau, C.M. Dobson, Amyloid fibril formation and seeding by wild-type human lysozyme and its disease-related mutational variants, J. Struct. Biol. 130 (2000) 339–351.
[11] R. Swaminathan, V.K. Ravi, S. Kumar, M.V. Kumar, N. Chandra, Lysozyme: A model protein for amyloid research, Adv. Protein Chem. Struct. Biol. 84 (2011) 63–111.
[12] G. Merlini, V. Bellotti, Lysozyme: a paradigmatic molecule for the investigation of protein structure, function and misfolding, Clin. Chim. Acta 357 (2005) 168–172.
[13] B. Lonnerdal, E.L. Lien, Nutritional and physiologic significance of alpha-lactalbumin in infants, Nutr. Rev. 61 (2003) 295–305.
[14] E.A. Permyakov, L.J. Berliner, α-Lactalbumin: structure and function, FEBS Lett. 473 (2000) 269–274.
[15] A. Häkansson, B. Zhivotovsky, S. Orrenius, H. Sabharwal, C. Svanborg, Apoptosis induced by a human milk protein, Proc. Natl. Acad. Sci. U.S.A. 92 (1995) 8064–8068.
[16] M. Svensson, H. Sabharwal, A. Hakansson, A.K. Mossberg, P. Lipniunas, H. Leffler, C. Svanborg, S. Linse, Molecular characterization of alpha-lactalbumin folding variants that induce apoptosis in tumor cells, J. Biol. Chem. 274 (1999) 6388–6396.
[17] P. Kopcansky, K. Siposova, L. Melnikova, Z. Bednarikova, M. Timko, Z. Mitroova, A. Antosova, V.M. Garamus, V.I. Petrenko, M.V. Avdeev, Z. Gazova, Destroying activity of magnetoferritin on lysozyme amyloid fibrils, J. Magn. Magn. Mater. 377 (2015) 267–271.
[18] H. Bloemendal, W. de Jong, R. Jaenicke, N.H. Lubsen, C. Slingsby, A. Tardieu, Ageing and vision: structure, stability and function of lens crystallins, Prog. Biophys. Mol. Biol. 86 (2004) 407–485.
[19] K.L. Moreau, J.A. King, Protein misfolding and aggregation in cataract disease and prospects for prevention, Trends Mol. Med. 18 (2012) 273–282.
[20] H. Ecroyd, J.A. Carver, Crystallin proteins and amyloid fibrils, Cell. Mol. Life Sci. 66 (2009) 62–81.
[21] J. Horwitz, Q.L. Huang, D. Linlin, M.P. Bova, Lens α-crystallin: chaperone-like properties, Meth. Enzymol. 290 (1998) 365–383.
[22] M. Garvey, H. Ecroyd, N.J. Ray, J.A. Gerrard, J.A. Carver, Functional amyloid protection in the eye lens: retention of α-crystallin molecular chaperone activity after modification into amyloid fibrils, Biomolecules 7 (67) (2017).
[23] K. Ulicna, Z. Bednarikova, W.-T. Hsuc, M. Holztragerova, J.W. Wue, S. Hamulakova, S.S.-S. Wang, Z. Gazova, Lysozyme amyloid fibrillization in presence of tacrine/acridone-coumarin heterodimers, Colloids Surf B Biointerfaces 166 (2018) 108–118.
[24] C. Dammers, D. Yolcu, L. Kukuk, D. Willbold, M. Pickhardt, E. Mandelkow, A.H.C.

Horn, H. Sticht, M.N. Malhis, N. Will, J. Schuster, S.A. Funke, Selection and Characterization of Tau Binding D-Enantiomeric Peptides with Potential for Therapy of Alzheimer Disease, PLoS ONE 22, 11 (12) e0167432.
[25] B. Raman, T. Ban, M. Sakai, S.Y. Pasta, T. Ramakrishna, H. Naiki, Y. Goto, C.M. Rao, αB-crystallin, a small heat-shock protein, prevents the amyloid fibril growth of an amyloid β-peptide and β2-microglobulin, Biochem. J. 392 (2005) 573–581.
[26] M.C. Daniel, D. Astruc, Gold nanoparticles: Assembly, supramole- cular chemistry, quantum-size-related properties, and applications toward biology, catalysis, and nanotechnology, Chem. Rev. 104 (2004) 293–346.
[27] M.J. Hostetler, J.E. Wintage, C.J. Zhong, J.E. Harris, R.W. Vachet, M.R. Clark, J.D. Londono, S.J. Green, J.J. Stokes, G.D. Wignall, G.L. Glish, M.D. Porter, N.D. Evans, R.W. Murray, Alkanethiolate gold cluster molecules with core diameters from 1.5 to 5.2 nm: core and monolayer properties as a function of core size, Langmuir 14 (1998) 17–30.
[28] S. Linse, C. Cabaleiro-Lago, W.F. Xue, I. Lynch, S. Lindman, E. Thulin, S.E. Radford, K.A. Dawson, Nucleation of protein fibrillation by nanoparticles, Proc. Natl. Acad. Sci. U.S.A. 104 (21) (2007) 8691–8696.
[29] D. Zhang, O. Neumann, H. Wang, V.M. Yuwono, A. Barhoumi, M. Perham, J.D. Hartgerink, P. Wittung-Stafshede, N.J. Halas, Gold nanoparticles can induce the formation of protein-based aggregates at physiological pH, Nano Lett. 9 (2) (2009) 666–671.
[30] A. Antosova, Z. Gazova, D. Fedunova, E. Valusova, E. Bystrenova, F. Valle, Z. Daxnerova, F. Biscarini, M. Antalik, Anti-amyloidogenic activity of glutathione-covered gold nanoparticles, Mater. Sci. Eng. C Mater. Biol. Appl. 32 (2012) 2529–2535.
[31] R.C. Triulzi, Q. Dai, J. Zou, R.M. Leblanc, Q. Gu, J. Orbulescu, Q. Huo, Photothermal ablation of amyloid aggregates by gold nanoparticles, Colloids Surf. B Biointerfaces 63 (2008) 200–208.
[32] S. Rocha, A.F. Thünemann, M.C. Pereira, M. Coelho, H. Möhwald, G. Brezesinski, Influence of fluorinated and hydrogenated nanoparticles on the structure and fibrillogenesis of amyloid beta-peptide, Biophys. Chem. 137 (2008) 35–42.
[33] Z. Bednarikova, P.D.Q. Huy, M.M. Mocanu, D. Fedunova, M.S. Li, Z. Gazova, Fullerenol C60(OH)16 prevents amyloid fibrillization of Aβ40 – In vitro and in silico approach, Phys. Chem. Chem. Phys. 18 (2016) 18855–18867.
[34] I.J. de Vries, W.J. Lesterhuis, J.O. Barentsz, P. Verdijk, J.H. van Krieken, O.C. Boerman, W.J. Oyen, J.J. Bonenkamp, J.B. Boezeman, G.J. Adema, J.W. Bulte, T.W. Scheenen, C.J. Punt, A. Heerschap, C.G. Figdor, Magnetic resonance tracking of dendritic cells in melanoma patients for monitoring of cellular therapy, Nat. Biotechnol. 23 (11) (2005) 1407–1413.
[35] T. Neuberger, B. Schöpf, H. Hofman, M. Hofman, B. von Rechenberg, Superparamagnetic nanoparticles for biomedical applications: possibilities and limitations of a new drug delivery system, J. Magn. Magn. Mater. 293 (2005) 483–496.
[36] A. Ito, M. Shinkai, H. Honda, T. Kobayashi, Medical application of functionalized magnetic nanoparticles, J. Biosci. Bioeng. 100 (1) (2005) 1–11.
[37] R. Hergt, R. Hiergeist, I. Hilger, W.A. Kaiser, Y. Lapatnikov, S. Margel, U. Richter, Maghemite nanoparticles with very high AC-losses for application in RF-magnetic hyperthermia, J. Magn. Magn. Mater. 270 (2004) 345–357.
[38] M. Mahmoudi, F. Quinlan-Pluck, M.P. Monopoli, S. Sheibani, H. Vali, K.A. Dawson, I. Lynch, Influence of the physiochemical properties of superparamagnetic iron oxide nanoparticles on amyloid β protein fibrillation in solution, ACS Chem. Neurosci. 20 (2013) 475–485.
[39] S. Sen, S. Konar, A. Pathak, S. Dasgupta, S. DasGupta, Effect of functionalized magnetic MnFe2O4 nanoparticles on fibrillation of human serum albumin, J. Phys. Chem. B 118 (2014) 11667–11676.
[40] H. Skaat, S. Margel, Synthesis of fluorescent-maghemite nanoparticles as multi-modal imaging agents for amyloid-beta fibrils detection and removal by a magnetic field, Biochem. Biophys. Res. Commun. 386 (4) (2009) 645–649.
[41] P. Wang, H. Konyoumdjian, D.C. Zhu, X. Huang, Heparin nanoparticles for β amyloid binding and mitigation of β amyloid associated cytotoxicity, Carbohydr. Res. 405 (2015) 110–114.
[42] A. Bellova, E. Bystrenova, M. Koneracka, P. Kopcansky, F. Valle, N. Tomasovicova, M. Timko, J. Bagelova, F. Biscarini, Z. Gazova, Effect of Fe3O4 magnetic nanoparticles on lysozyme amyloid aggregation, Nanotechnology 21 (2010) 6 065103.
[43] K. Siposova, K. Pospiskova, Z. Bednarikova, I. Safarik, M. Safarikova, M. Kubovcikova, P. Kopcansky, Z. Gazova, The molecular mass of dextran used to modify magnetite nanoparticles affects insulin amyloid aggregation, J Magn Magn Mater 427 (2017) 48–53.
[44] K. Siposova, M. Kubovcikova, Z. Bednarikova, M. Koneracka, V. Zavisova, A. Antosova, P. Kopcansky, Z. Daxnerova, Z. Gazova, Depolymerization of insulin amyloid fibrils by albumin -modified magnetic fluid, Nanotechnology 23 (2012) 10 055101.
[45] V. Zavisova, M. Koneracka, J. Kovac, M. Kubovcikova, I. Antal, P. Kopcansky, M. Bednarikova, M. Muckova, The cytotoxicity of iron oxide nanoparticles with different modifications evaluated in vitro, J Magn Magn Mater 380 (2015) 85–89.
[46] I. Antal, M. Koneracka, M. Kubovcikova, V. Zavisova, I. Khmara, D. Lucanska, L. Jelenska, I. Vidlickova, M. Zatovicova, S. Pastorekova, N. Bugarova, M. Micusik, M. Omastova, P. Kopcansky, D, L-Lysine functionalized F_e3_O4 nanoparticles for detection of cancer cells, Colloids Surf. B Biointerfaces 163 (2018) 236–245.
[47] J.T. Woods, M.G. Mellon, Thiocyanate method for iron-spectrophotometric method, Ind Eng Chem 13 (1941) 551–554.
[48] H. Meyer, The ninhydrin reaction and its analytical applications, Biochem. J. 67 (2) (1957) 333–340.
[49] E. Tombácz, A. Majzik, Zs. Horvát, E. Illés,, The thicker coating provides better stability, especially in the case of magnetic, Rom Rep Phys 58 (2006) 281–286.
[50] N.C. Feitozaa, T.D. Gonçalvesa, J.J. Mesquita, Fabrication of glycine-functionalized maghemite nanoparticles for magnetic removal of copper from waste water, J. Hazard. Mater. 264 (2014) 153–160.
[51] K. Dubey, B.G. Anand, R. Badhwar, G. Bagler, P.N. Navya, H.K. Daima, K. Kar, Tyrosine- and tryptophan- coated nanoparticles inhibit amyloid aggregation of insulin, Amino Acids 47 (2015) 2551–2560.